NUMERICAL SIMULATION AND APPLICATION OF ARGON BLOWING FROM TUNDISH COVER FOR BLOOM CONTINUOUS CASTING

C.-H. Wu [a,*], Y. Li [a], Y.-D. Liu [a], X. Xie [a], G.-R. Wu [b], M. Zhang [a]

[a] Institute of Materials Engineering & Technology, Pangang Group Research Institute Co., Ltd., Sichuan, China
[b] Steel Research Institute for Automobile and Household Appliances, Pangang Group Research Institute Co., Ltd., Sichuan, China

Abstract

During the continuous casting process, the residual oxygen in the tundish can be significantly reduced by argon blowing from the tundish cover (ABTC). As a result, the effect of protective casting can be obviously improved, which helps to reduce the reoxidation of molten steel in the tundish. In the present work, numerical models for the ABTC of a six-strand continuous casting machine were established and verified by the measured oxygen mass fraction in the tundish during the ABTC. The results indicate that the best conditions for ABTC are to install the argon pipes on either side of the tundish cover holes, seal the baking holes, and keep the stopper rod holes open. The argon flow rate should be ≥120 m³/h during the period of empty tundish and ≥60 m³/h during the period of normal casting. Based on the calculation results, industrial testsof ABTC were carried out. The results indicated that the increased nitrogen content in steel($\Delta_{w[N]}$) decreased by 21.5% from 8.78×10⁻⁶ to 6.89×10⁻⁶ , from the end of RH to tundish, and the amount of inclusions except for MnS in bloom (scanned size: 8 mm × 8 mm) decreased by 21.3% from 13.43 to 10.57, and the average size of inclusions decreased by 19.0% from 9.27 μm to 7.51 μm.

1. Introduction

With the rapid development of transportation, national defense, and marine engineering, high purity has become the development direction of advanced steel materials [1-4] in recent years. The cleanliness of molten steel can be greatly improved after the refining process of LF, RH, etc. However, if the effect of protective casting in the tundish during the subsequent continuous casting process is poor, reoxidation of the molten steel can easily occur [5] leading to a bad influence on the cleanliness of molten steel.

Argon is a protective gas that is widely used in the industry of steel production. During the continuous casting process, argon was applied during argon seal for ladle shroud [6-8] and submerged entry nozzle (SEN) [9,10], argon blowing through the stopper rod or the upper nozzle of tundish [11-13] and the argon bubbling curtain in tundish [14-16]. These technologies significantly improve the process stability and steel cleanliness. Additionally, the argon blowing to tundish plays an important role in improving the cleanliness of the molten steel. During this process, argon is blown into the tundish through argon pipes installed in the tundish cover or elsewhere in the tundish, and the air in the tundish is then discharged. As a result, the protective casting effect can be significantly improved when the remaining oxygen in tundish drops below 1% [17]. Experimental results by Story, et al. [18] showed that the loss of acid-soluble aluminum (Δ_w[Al]s) of steel could be significantly reduced by 87.5% by argon blowing into the tundish. Considering the advantages of argon blowing into the tundish, some plants in Europe and Japan have adopted this process and achieved good application effects [19]. In these plants, the defect rate of IF steel in Corus decreased by 38%, and the amount of inclusion in continuous casting steel along the casting direction in POSCO significantly decreased. Currently, some plants [20-23] in China have also adopted this process, with the clogging rate of SEN in Han Steel [20, 21] decreasing from 8% to 3%, and the surface defect rate of deep drawing component in one plant [23] decreased from 7.8% to 2.6%.

The previous studies on argon blowing into tundish were mainly conducted on an experimentalbasis. To determine rational parameters of argon blowing into tundish, plant trials should be conducted repeatedly, which prolongs the trial cycle and increases the trial costs. Considering this, Li [24]

first conducted a numerical investigation on argon blowing into tundish for a two-strand slab continuous casting machine, and successfully developed and applied the process of argon blowing into tundish based on the numerical calculation results. Compared to the slab continuous casting machine, the tundish structure of the bloom continuous casting machine differs considerably. The tundish of a bloom continuous casting machine generally has a much smaller volume and more stopper rod holes (corresponding to the different strands). As a result, the gas flow and the gas content variation in the tundish during argon blowing into tundish also differ significantly between slab and bloom continuous casting machine. In the present work, the argon blowing from tundish cover (ABTC) for a six-strand bloom continuous casting machine was firstly investigated numerically. The variation of the gas content in the tundish under different conditions, including the installation of argon pipes, the sealing method of tundish cover holes, and the argon flow rate, were calculated and discussed. Based on the calculation results the best conditions of ABTC were determined . Plant trials of ABTC for the six-strand bloom continuous casting machine were then successfully carried out.

2. Numerical Simulation of ABTC
2.1. Numerical models
2.1.1. Model description

The investigated tundish is a T-type one with 6 strands as shown in Figure 1 and Figure 2. The tundish cover includes 6 stopper rod holes (S1~S6) and 5 baking holes (B1~B5). The left and right parts of the tundish are the casting area, and the center part is the pouring area. ABTC can be implemented by blowing argon into the tundish through argon pipes installed in the cover. a1~a11, b1~b11, and c1~c11 in Figure 2 are the involved location of argon pipes in the following calculation. The argon can be blown through argon pipes, as shown by the red arrow lines in the downward direction in Figure 1. Meanwhile, the air in the tundish can be discharged from S1~S6

and B1~B5 if these holes are not sealed, as shown by black arrow lines in the upward direction in Figure 1. Table 1 lists the process parameters and the physical properties of the gas.

In the initial stage of casting in the tundish, the covering flux on the surface of the molten steel cannot be fully melted immediately, and thus reoxidation of the molten steel due to the remaining oxygen in the tundish occurs easily. Although the covering flux can be fully melted during the subsequent period of normal casting, the melted covering flux on the molten steel surface sometimes forms solidified crust [25-27] due to the influence of the stuffing sand, inclusion floatation, and refractory erosion, etc. As a result, reoxidation of the molten steel easily occurs at the place where the solidified crust of the covering fluxhas formed.

Therefore, it is necessary to implement ABTC to discharge the air in the tundish during the period of empty tundish before casting, and it is also necessary to implement ABTC during the subsequent period of normal casting to maintain a low level (<1%) of oxygen content. Considering this, the inner cavity of half of the tundish was taken towards its width to develop the numerical calculation models for ABTC during the period of empty tundish (Figure 3(a)) and the subsequent period of normal casting (Figure 3(b)). During the period of normal casting, only the space between the molten steel surface and the tundish cover contains gas. Therefore, the volume of the model in Figure 3(b) is significantly smaller than that in Figure 3(a). Octahedral grids were adopted to mesh the numerical models and the model in Figure 3(a) and Figure 3(b) contains 355078 and 277164 grids respectively. The following assumptions were made in the modelling:

(1) The temperature of the blown argon into the tundish rose immediately to the inner temperature of the tundish.

(2) The temperature distribution of the tundish inner cavity was uniform, and the inner temperature of the tundish during the period of empty tundish and normal casting was 1200 °C and 1500 °C respectively based on the measured values.
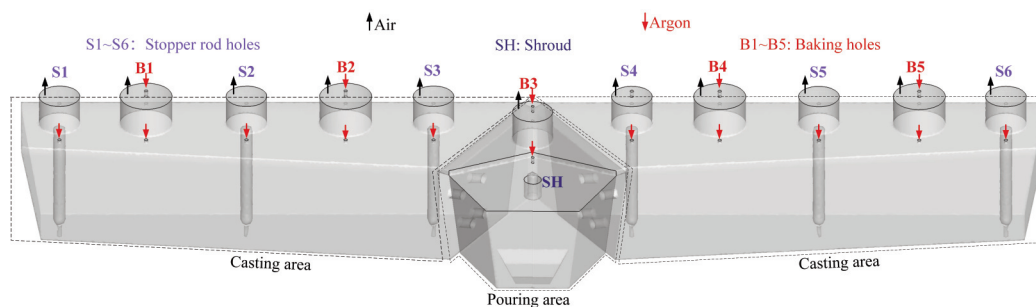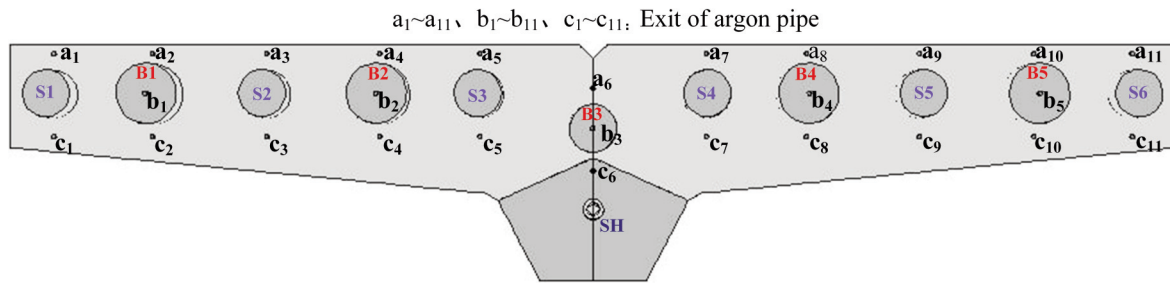

Figure 1. 3D view of tundish inner cavity

$a_1 \sim a_{11}$、 $b_1 \sim b_{11}$、 $c_1 \sim c_{11}$：Exit of argon pipe

Figure 2. Vertical view of tundish inner cavity

Table 1. Process parameters and physical properties of the gas

| Item	Value
Nominal capacity /t	40
Bloom section size /mm×mm	280×325 280×380
Casting speed /m·min^{-1}	0.62~0.75
Depth of molten steel during normal casting period /mm	900
Diameter of shroud /mm	90
Submerged depth of shroud /mm	350
Diameter of stopper rod /mm	130
Diameter of baking hole /mm	320
Diameter of argon pipe /mm	15
Distance between molten steel surface and tundish cover /mm	150
Density of argon in 298 K /kg·m^{-3}	1.568
Density of air in 298 K /kg·m^{-3}	1.184
Viscosity of argon /kg·m^{-1}·s^{-1}	2.125×10^{-5}
Viscosity of air /kg·m^{-1}·s^{-1}	1.789×10^{-5}
Volume fraction of oxygen in air	0.21
Mass diffusivity of mixture /m^2·s^{-1}	2.88×10^{-5}
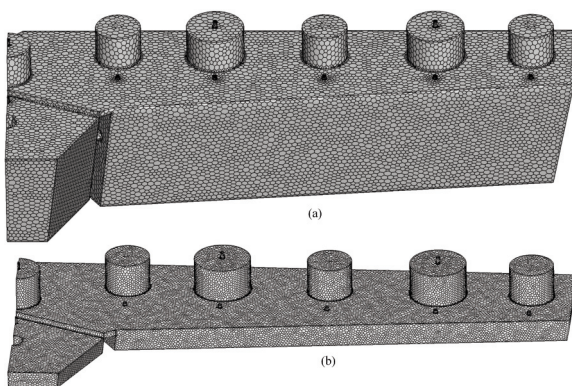
Figure 3. Models of ABTC during (a) period of empty tundish and (b) period of normal casting

(3) The temperature variation of the tundish inner cavity during ABTC was ignored due to the low specific heat capacity of argon.

(4) The variation of volume and density of the blown argon into tundish due to the temperature rise could be determined by the ideal gas equation.

(5) The remaining gas in the tundish was regarded as incompressible.

In the modeling, argon pipes were defined as velocity inlets through which the argon was blown into the computational domain. The baking holes, which were connected to the atmosphere, were defined as pressure outlets with arelative static pressure of 0 Pa. Air was assumed to be the back-flow gas generated near the outlet. All surfaces except the argon pipes and the baking holes were assumed to have non-slip wall boundary conditions. At the beginning of ABTC, the tundish was filled with air. SIMPLEC was chosen as the solving algorithm for the simulation. The time step during the calculation was 0.05 s, and the calculation convergence was <10^{-4} for all residuals.

2.1.2. Governing equations and boundary conditions

The flow and content variation of gas in the tundish during ABTC can be described by governing equations as follows.

(1) Continuity equation

$$\frac{\partial \rho}{\partial t} + \nabla \cdot (\rho \boldsymbol{u}) = 0 \qquad (1)$$

Where, ρ is the density of mixed gas, kg/m³; t is time, s; u is velocity, m/s.

(2) Momentum conservation equation

$$\frac{\partial}{\partial t}(\rho \boldsymbol{u}) + \nabla \cdot (\rho \boldsymbol{uu}) = -\nabla P + \qquad (2)$$

$$\nabla \cdot (\mu_{eff} \nabla \boldsymbol{u}) + \rho \boldsymbol{g}$$

$$\mu_{eff} = \mu + \mu_t = \mu + \rho C_\mu \frac{k^2}{\varepsilon} \qquad (3)$$

Where, P is pressure, Pa; g is gravity acceleration, m/s²; μ and μ_t are molecular and turbulent viscosities respectively, Pa·s.

(3) Turbulent equations

Turbulence can be described by the k-ε model [28], which includes the equation describing turbulent kinetic energy (k) and the equation describing the dissipation rate of turbulence energy (ε):

$$\frac{\partial(\rho k)}{\partial t} + \nabla \cdot (\rho \boldsymbol{u} k) =$$

$$= \nabla \cdot \left[\left(\mu + \frac{\mu_t}{\sigma_k} \right) \nabla k \right] + G_k - \rho \varepsilon \qquad (4)$$

$$\frac{\partial(\rho \varepsilon)}{\partial t} + \nabla \cdot (\rho \boldsymbol{u} \varepsilon) = \nabla \cdot \left[\left(\mu + \frac{\mu_t}{\sigma_\varepsilon} \right) \nabla \varepsilon \right] +$$

$$\frac{\varepsilon}{k} (C_1 G_k - C_2 \rho \varepsilon) \qquad (5)$$

Where, C_1, C_2, C_μ, σ_k, σ_ε are the empirical constants with the value of 1.44, 1.92, 0.09, 1.0, and 1.3 respectively; Gk is the generated turbulence kinetic energy due to the mean velocity gradients, m²/s². (4) Species transport equation

$$\frac{\partial}{\partial t}(\rho Y_i) + \nabla \cdot (\rho \boldsymbol{u} Y_i) = -\nabla \boldsymbol{J} \qquad (6)$$

Where Y is the mass fraction; i represents argon or air in the tundish, and the mass fraction of oxygen in the air is 23.3%.

During the calculation, the velocity of the blown argon at the outlet of the argon pipes was taken as the boundary condition. The inner surface of the tundish was regarded as a non-slip surface, and the relative static pressure at the outlet of the stopper rod holes and baking holes was set as 0 Pa. The SIMPLE algorithm was adopted for the calculation model, and the calculation convergence was considered to be achieved when the normalized residuals were smaller than 10^{-4} [29].

2.1.3. Model validation

To verify the calculation model, ABTC with different argon flow rates was carried out when the tundish was empty, during which the inner temperature of the tundish was ~1200 °C after it was baked before continuous casting began. The oxygen mass fraction was measured by the Optima 7 gas analyzer. During the ABTC, argon pipes (a1~a11 c1~c11) were installed on either side of the tundish cover holes with baking holes (B1~B5) sealed. Figure 4 compares the measured mass fraction of oxygen in tundish with the calculated values. It can be seen that the calculated mass fraction of oxygen continuously decreases during the ABTC and that the mass fraction of oxygen with a larger argon flow rate of 120 m³/h is significantly smaller than that with an argon flow rate of 80 m³/h. The calculated results agree well with the measured ones, and the relative error is less than 6.5%.
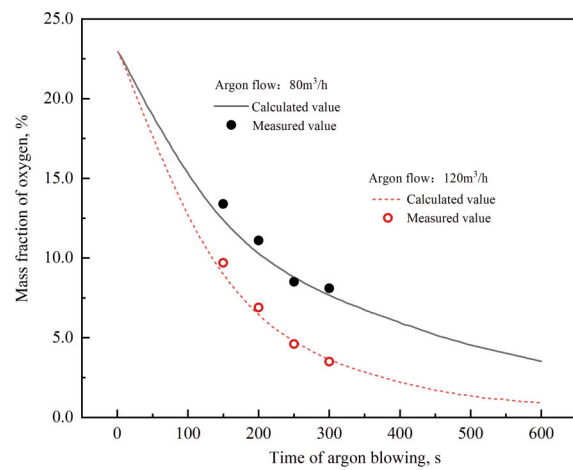

Figure 4. The calculated and measured mass fraction of oxygen during ABTC

To evaluate the applicability of the grid size, different grid sizes, corresponding to different grid quantity (G1~G4), was applied for meshing the calculation domain of the model during the period of empty tundish (Figure 3(a)). The mass fraction of oxygen during ABTC was then calculated with an

argon flow of 120 m³/h. The other calculation conditions were the same as mentioned at the beginning of this section.

Table 2 compares the calculation results and the relative errors with G1~G4 after 300 s of ABTC. The errors decrease with the increase of grid quantity from G1 to G4. For G3, the relative error (δ_{oxygen}) to G4 (the finest grid) is 3.42%, which meets the requirement of

scheme is similar. In the initial stage, the air in tundish can be efficiently discharged thanks to the blown argon, and thus the mass fractions of air and oxygen decrease rapidly. As the ABTC progresses, the concentration of the remaining air and oxygen in the tundish continuously decreases, and so does the concentration of the discharged air and oxygen from the tundish. Meanwhile, the external air can enter the

Table 2. Error statistics of different meshes

Grid	G1	G2	G3	G4
Total grid number	186248	269346	355078	432654
Total node number	1074279	1553589	2048091	2495550
Average mass faction of oxygen	0.0385	0.0377	0.0363	0.351
$\delta_{oxygen} = |F_{oxygen-i} - F_{oxygen-4}|/F_{oxygen-4}$	0.0972	0.0733	0.0342	–

computational accuracy. Therefore, in order to reduce the computational cost and improve computational efficiency, G3 was selected for modeling.

2.2. Results and discussion

2.2.1. Calculation for installation location of argon pipes and seal method of tundish cover holes during the period of empty tundish

During the practical production, approximately 5~10 minutes elapse between the end of tundish baking and the start of casting for tundish. During this time, the effect of ABTC is closely related to the installation location of the argon pipes and the sealing method of the tundish cover holes. To determine the best conditions of ABTC, seven schemes for ABTC during the period of empty tundish were designed and shown in Table 3. The gas content within 10 minutes during ABTC for different schemes was calculated. The schemes in Table 2 can be divided into two groups based on the installation of argon pipes, and the argon flow rate in each scheme is 100 m³/h.

tundish through tundish cover holes. As a result, the mass fraction of air and oxygen in the tundish decreases more and more slowly and nearly reaches a stable value in the later stage.

To compare the effect of ABTC with schemes 1~4, the mass fraction of the remaining oxygen in the tundish with different schemes after 240 s, 360 s, 480 s, and 600 s was compared in Figure 6. Compared with Scheme 1, the mass fraction of remaining oxygen in the tundish decreases in the same time with cover holes sealed in Scheme 2~4, which means that the effect of ABTC is improved with cover holes sealed in Scheme 2~4. In particular, in Scheme 4, the mass fraction of remaining oxygen in the tundish is much lower than that with Scheme 1~3. After implementing ABTC for 600 s with Scheme 1~4, the mass fraction of remaining oxygen in tundish is 13.7%, 12.1%, 8.3%, and 2.5% respectively. The mass fraction of remaining oxygen with Scheme 4 decreases by 81.8%, 79.3%, and 69.9% compared with Scheme 1~3, respectively.

Table 3. Schemes of ABTC during the period of empty tundish

Group No.	Scheme No.	The installation location of argon pipes	Seal method of tundish cover holes
1#	1	b1~b5	/
	2	b1~b5	S1-S6
	3	b1~b5	B1-B5
	4	b1~b5	S1-S6; B1-B5
2#	5	a1-a11 c1-c11	S1-S5
	6	a1-a11 c1-c11	B1-B5
	7	a1-a11 c1-c11	S1-S6; B1-B5

Figure 5 shows the mass fraction variation of air and oxygen during the ABTC according to schemes 1~4. The variation trend of gas content in each

In Scheme 1~4, the argon pipes are installed in the baking holes of the tundish cover, which is convenient for argon pipes installation. However, the calculated
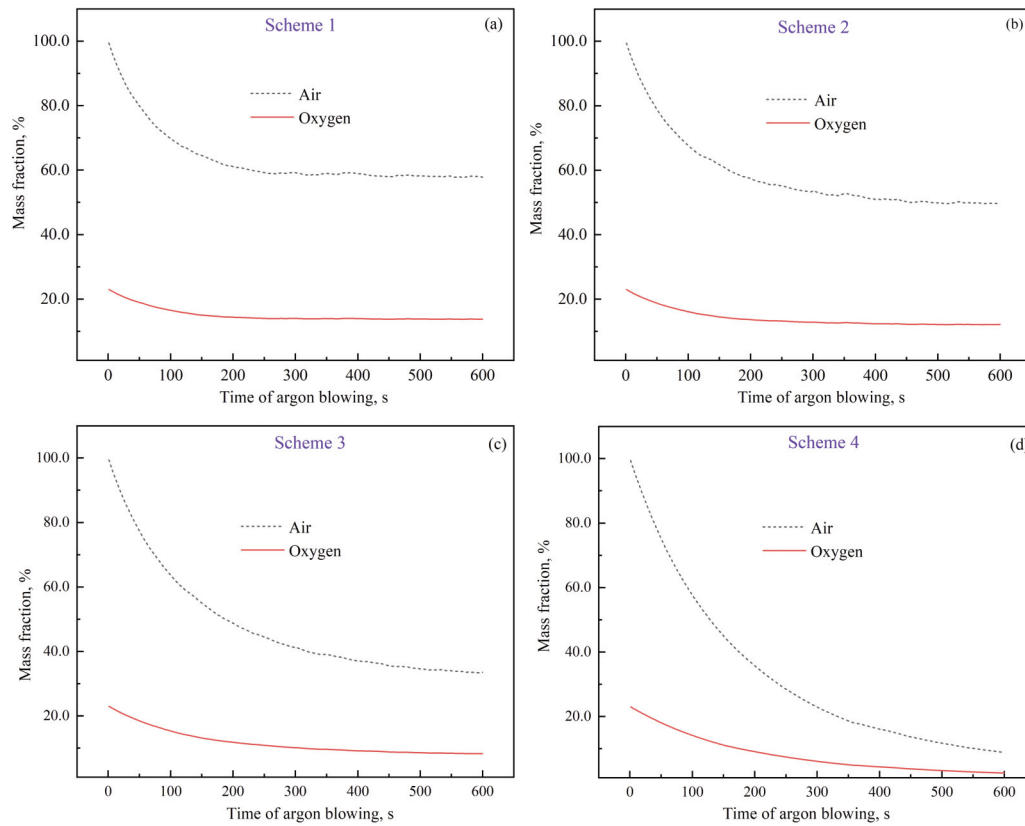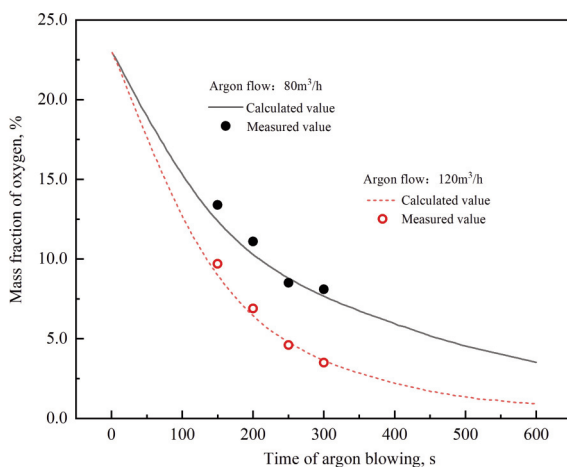
Figure 5. *Variation of gas content in tundish during ABTC with (a)Scheme 1, (b) Scheme 2, (c) Scheme 3, and (d) Scheme 4*

results shown in Figure 7 indicate that some blown argon can directly escape from the tundish and that air can be easily sucked into the tundish from the exit of the baking holes when argon pipes are installed in the baking holes. As a result, the effect of ABTC with Scheme 1~4 is slightly affected during the practical

Figure 6. *Mass fraction of remaining oxygen in tundish with Scheme 1~4 after different times of argon blowing*

production. Considering this, Scheme 5~7 was also designed with argon pipes installed on both sides of the tundish cover holes, as shown in Table 2.

Figure 8 shows the mass fraction of remaining oxygen in tundish with Scheme 4~7 after different times of argon blowing. Compared to Scheme 4, the mass fraction of remaining oxygen with Scheme 5~7 is lower. This means that the air in tundish can be discharged more efficiently with the argon pipes moved from the baking holes to both sides of the tundish cover holes. As a result, the efficiency of ABTC can be improved. Compared to Scheme 5 and Scheme 7, the mass fraction of remaining oxygen in the tundish is lower in Scheme 6. This indicates that the baking holes should be sealed with stopper rod holes open when argon pipes are installed on both sides of the tundish cover holes for obtaining a better effect of ABTC.

Based on the analysis above, to obtain a better effect of ABTC during the period of empty tundish, both baking holes and stopper rod holes should be sealed when argon pipes are installed in the baking holes (Scheme 4), and the baking holes should be sealed with stopper rod holes open when the argon pipes are installed on both sides of the tundish cover holes (Scheme 6).
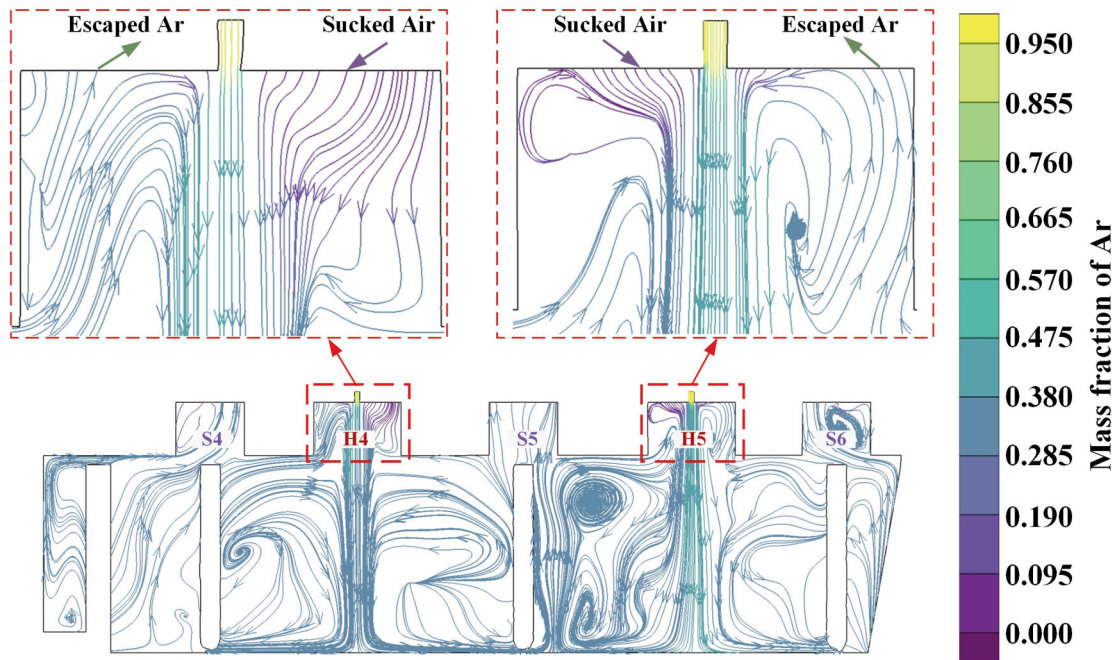
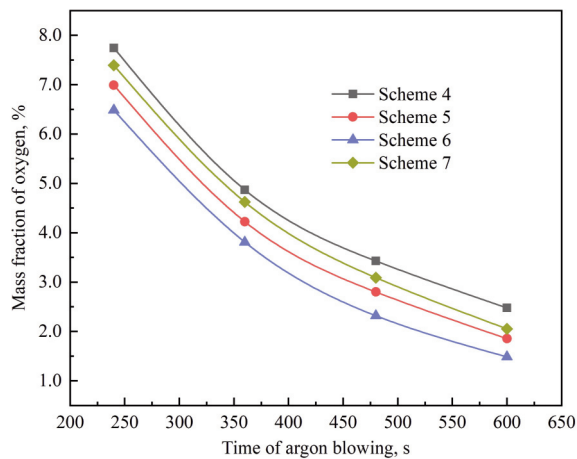*Figure 7. Streamlines during ABTC with Scheme 1*

Figure 8. *Mass fraction of remaining oxygen in tundish with Scheme 4~7 after different times of argon blowing*

2.2.2. Calculation for argon flow rate during the period of empty tundish

It is determined from the analysis in Section 2.2.1 that the effect of ABTC with Scheme 4 and Scheme 6 is better if argon pipes are installed in the baking hole and installed or on both sides of the tundish cover, respectively. To further determine the rational argon flow rate, the mass fraction of remaining oxygen in the tundish was calculated at different argon flow rates for Scheme 4 and Scheme 6, respectively. Figure 9 shows the calculation results. In both Scheme 4 and

Scheme 6, the mass fraction of remaining oxygen decreases as the argon flow rate increases. However, the mass fraction of remaining oxygen decreases more slowly with continuously increasing argon flow rate. This indicates that the efficiency of ABTC continuously decreases as the argon flow rate increases.

To effectively protect the molten steel in the tundish from reoxidation due to the remaining oxygen, the mass fraction of the remaining oxygen should be maintained below 1% [17] with ABTC. The maximum argon flow rate that can be provided in practical production is ~130 m^3/h. Under the condition of this maximum argon flow rate, the mass fraction of remaining oxygen in the tundish after implementing ABTC for 600 s with Scheme 4 and Scheme 6 is 1.7% and 0.7%, respectively. This means that the mass fraction of remaining oxygen in tundish cannot meet the requirement of <1% if ABTC is implemented with Scheme 4. Therefore, Scheme 6 is the best solution, and the mass fraction of remaining oxygen in the tundish can decrease to 0.95% after argon blowing for 600 s with an argon flow rate of 120 m^3/h.

2.2.3. Calculation for argon flow rate during the period of normal casting

Compared with the period of the empty tundish, the holding capacity of gas in the tundish between the molten steel surface and the tundish cover decreases sharply during the period of normal casting. As a
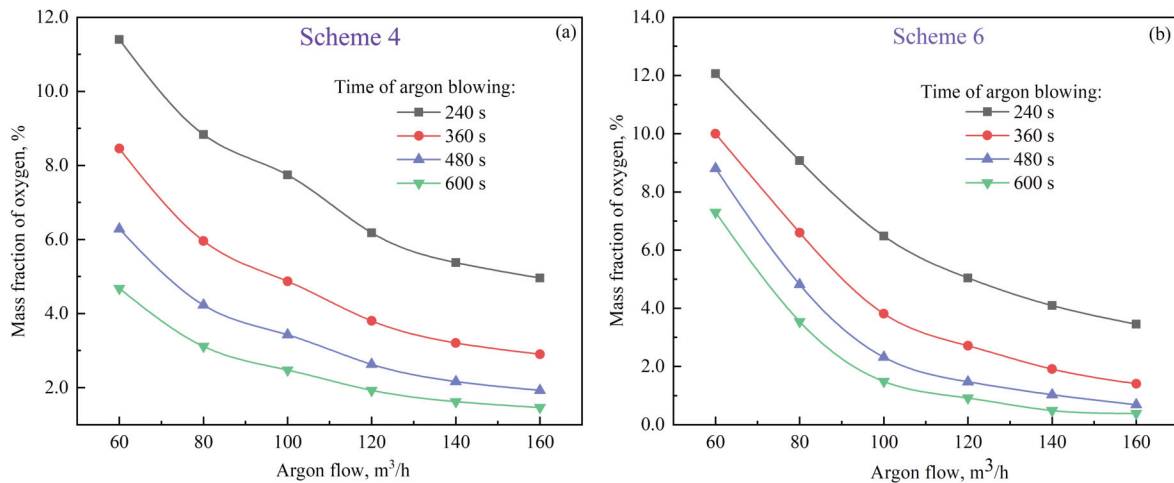
Figure 9. Variation of mass fraction of remaining oxygen in tundish with different argon flow rates by applying (a) Scheme 4 and (b) Scheme 6

result, the argon flow rate of ABTC should be adjusted during the period of normal casting. In view of this, the mass fraction of remaining oxygen in the tundish was calculated using Scheme 6 with the calculation model shown in Figure 3(b) under the condition of different argon flow rates. In the calculation, the mass fraction of remaining oxygen after argon blowing for 5 minutes was taken as the initial condition.

Figure 10 shows the calculation results. As the time of argon blowing increases, the mass fraction of oxygen in the tundish continuously decreases and finally reaches a relatively stable value. The final stable value presents a downtrend with the argon flow rate increased. Under the condition of the argon flow rate of 50 m³/h and 60 m³/h, the final mass fraction of remaining oxygen in the tundish can reach 1.1% and 0.8%, respectively. Therefore, the argon flow rate should be ≥60 m³/h to keep the mass fraction of

remaining oxygen in tundish below 1% during the period of normal casting.

3. Industrial application

To evaluate the effect of ABTC, two consecutive tundishes were used for the experiment during the practical continuous casting. Each tundish continuously cast 18 heats. The first tundish without ABTC served as the control group and the second tundish with ABTC (Scheme 6) served as the trial group. Figure 11 shows the ABTC during continuous casting with the second tundish. The process parameters during the trials are listed in Table 4.

During the trials, steel samples in end of RH and in the tundish for each heat were taken. The nitrogen content of the steel samples was measured and shown in Table 5. By applying ABTC, the average nitrogen
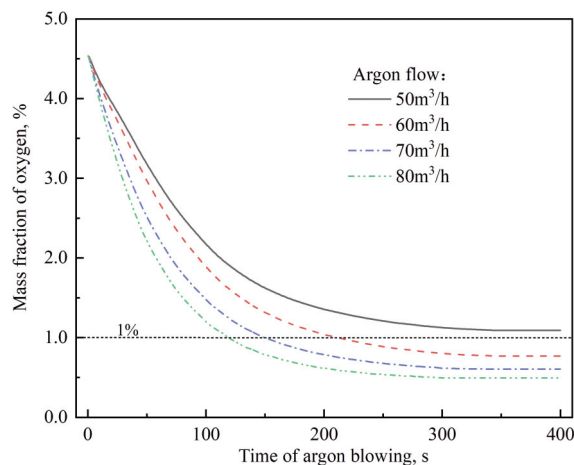

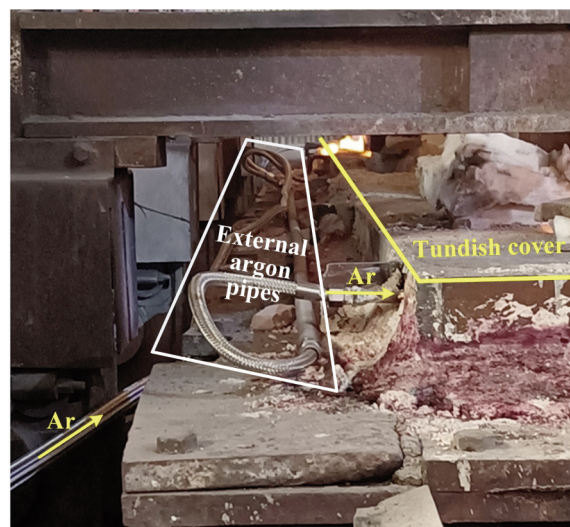*Figure 10. Mass fraction of remaining oxygen in tundish with different argon flow rate*

Figure 11. Industrial trial of ABTC

Table 4. Process parameters during the trials

Item	Value
ABTC during the period of empty tundish	Argon flow rate: 130 m³/h Time of argon blowing: 6 minutes
ABTC during the period of normal casting	Argon flow rate: 60 m³/h Time of argon blowing: all the time
Steel grade	U75V
Steel composition /wt%	C:0.7~0.8 Si:0.6~0.8 Mn:0.8~1.0 P:<0.02 S: <0.015
Casting speed /m·min⁻¹	0.7
Section size /mm×mm	280×380

Table 5. Mass faction of nitrogen of steel samples in end of RH and in the tundish

Heat No.	The trial group with ABTC /×10⁻⁶			The control group without ABTC /×10⁻⁶		
	End of RH	Tundish	$\Delta[N]$	End of RH	Tundish	$\Delta[N]$
1	33	43	10	37	51	14
2	36	42	6	35	47	12
3	42	47	5	40	49	9
4	41	48	7	38	49	11
5	34	41	7	33	43	10
6	39	46	7	41	47	6
7	40	45	5	42	49	7
8	39	48	9	41	49	8
9	40	45	5	35	45	10
10	37	43	6	41	48	7
11	36	45	9	37	48	11
12	32	40	8	30	42	12
13	44	48	4	45	51	6
14	38	44	6	35	42	7
15	37	42	5	38	44	6
16	39	45	6	41	47	6
17	36	45	9	35	42	7
18	34	44	10	37	46	9
Average	37.61	44.5	6.89	37.83	46.61	8.78
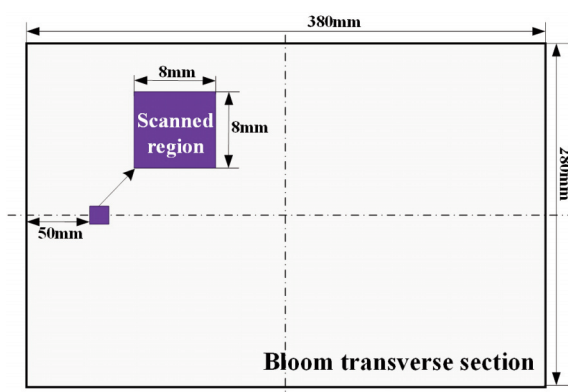
Figure 12. Scanned region in the bloom transverse section

content of the steel samples in the tundish decreases from $46.6×10^{-6}$ to $37.8×10^{-6}$, and the increased nitrogen content ($\Delta_{w[N]}$) from the end of RH to the tundish decreases by 21.5% from $8.78×10^{-6}$ to $6.89×10^{-6}$. This indicates that the reoxidation of molten steel in the tundish caused by the remaining oxygen can be significantly decreased and the protective casting in the tundish can be thus enhanced.

Inclusions with a size of >3 μm in steel samples were examined with the ASPEX automatic scanning electron microscope. The scanned area, as shown in Figure 12, is an 8 mm × 8 mm square located 50 mm from the center of the narrow surface of the bloom. The MnS inclusions are formed during the solidification process, which is not related to the re-

Table 6. Scan results of inclusions (except for MnS) in bloom

Heat No.	The trial group with ABTC		The control group without ABTC	
	Amount	Average size /μm	Amount	Average size /μm
1	14	7.5	17	9.7
4	12	6.9	13	9.1
7	10	6.5	12	8.2
10	9	8.4	14	8.8
13	11	7.6	11	9.2
15	10	7.4	15	9.5
18	8	8.3	12	10.4
Average value	10.6	7.5	13.4	9.3

oxidation in the tundish during continuous casting. For this reason, only the inclusions other than MnS were analyzed, and the analysis results are listed in Table 6. Compared to the control group without ABTC, the average amount of inclusions with ABTC in the trial group decreases by 21.3% from 13.43 to 10.57, and the average size of inclusions decreases by 19.0% from 9.27 μm to 7.51 μm.

4. Conclusions

(1) To obtain a better effect of ABTC, stopper rod holes and baking holes should be sealed when argon pipes are installed in the baking holes (Scheme 4), and the baking holes should be sealed with stopper rod holes open when argon pipes are installed on both sides of the cover holes (Scheme 6).

(2) Scheme 6 was selected as the best conditions for implementing ABTC based on the maximum argon flow rate that could be supplied during practical production. The argon flow rate should be ≥120 m^3/h during the period of the empty tundish and ≥60 m^3/h during the period of normal casting.

(3) Plant trials of ABTC with Scheme 6 were carried out. The trials results showed that the increased nitrogen content ($\Delta_{w[N]}$) decreased by 21.5% from 8.78×10^{-6} to 6.89×10^{-6} from the end of RH to the tundish, and the amount of inclusions except for MnS in bloom (Scanned size: 8 mm × 8 mm) decreased by 21.3% from 13.43 to 10.57. At the same time, the average size of the inclusions decreased by 19.0% from 9.27 μm to 7.51 μm.

Authors' contributions

Chen-hui Wu: Designing schemes of ABTC; Analysing data; writing original draft.

Yang Li and Xin Xie: conducting numerical simulation.

Ying-dong Liu: Designing and manufacturing the tundish cover for argon blowing.

Guo-rong Wu and Min Zhang: conducting plant trials and examining the samples.

Declaration of Competing Interest

The authors declare that they have no known competing financial interests or personal relationships that could have appeared to influence.

Data Availability Statement

The data in the present work for reproducing these findings cannot be shared at this time, because these data are also part of our ongoing study.

References

[1] K.D. Kuang, Certain basic subjects on clean steel, Acta Metallurgica Sinica, 45(3) (2009) 257-269. https://doi.org/10.3321/j.issn:0412-1961.2009.03.001.

[2] Y. Sahai, Tundish technology for casting clean steel: a review, Metallurgical and Materials Transactions B, 47(4) (2016) 2095-2106. https://doi.org/10.1007/s11663-016-0648-3

[3] J. Zhang, J.H. Liu, S.J. Yu, D.X. Dong, G.L. Wang, S.Q. Li, Production of clean steel using the nitrogen elevating and reducing method, Metals, 8(7) (2018) 560. https://doi.org/10.3390/met8070560

[4] B.A. Webler, P.C. Pistorius, A review of steel processing considerations for oxide cleanliness, Metallurgical and Materials Transactions B, 51(6) (2020) 2437-2452. https://doi.org/10.1007/s11663-020-01949-y

[5] K. Sasai, Y. Mizukami, Reoxidation behavior of molten steel in tundish, ISIJ International, 40(1) (2000) 40-47. https://doi.org/10.2355/isijinternational.40.40

[6] J.S. Zhang, L. Qing, S.F. Yang, Z.X. Chen, J.S. Li, Z.Y. Jiang, Advances in ladle shroud as a functional device in tundish metallurgy: A review, ISIJ International, 59(7) (2019) 1167-1177. https://doi.org/10.2355/isijinternational.ISIJINT-2019-044

[7] S. Chatterjee, D.H. Li, K. Chattopadhyay, Tundish open eye formation: a trivial event with dire consequences, Steel Research International, 88(9) (2017) 1600436. https://doi.org/10.1002/srin.201600436

[8] S. Chatterjee, D.H. Li, K. Chattopadhyay, Modeling of liquid steel/slag/argon gas multiphase flow during tundish open eye formation in a two-strand tundish, Metallurgical and Materials Transactions B, 49(2)

(2018) 756-766.
https://doi.org/10.1007/s11663-018-1177-z

[9] Q.R. Lai, Z.G. Luo, Q.F. Hou, T. Zhang, X.A. Wang, Z.S. Zou, Numerical study of inclusion removal in steel continuous casting mold considering interactions between bubbles and inclusions, ISIJ International, 58(11) (2018) 2062-2070.
https://doi.org/10.2355/isijinternational.ISIJINT-2018-319

[10] Z.Q. Liu, B.K. Li, A. Vakhrushev, M.H. Wu, A. Ludwig, Physical and numerical modelling of exposed slag eye in continuous casting mold using Euler-Euler approach, Steel Research International, 90(4) (2019) 1800117. https://doi.org/10.1002/srin.201800117

[11] F.G. Liu, H.C. Zhou, L.F. Zhang, C.Y. Ren, J. Zhang, Y. Ren, W. Chen, Effect of temperature and multichannel stopper rod on bubbles in water model of a steel continuous caster, Steel Research International, 92(9) (2021) 2100067.
https://doi.org/10.1002/srin.202100067

[12] Y. Li, C.G. Cheng, M.L. Yang, Z.X. Dong, Z.L. Xue, Behavior characteristics of argon bubbles on inner surface of upper tundish nozzle during argon blowing process, Metals, 8(8) (2018) 590.
https://doi.org/10.3390/met8080590

[13] X.F. Qin, C.G. Cheng, Y. Li, W.L. Wu, J. Yan, Effects of argon blowing at tundish upper nozzle on multiphase flow behavior in nozzle, Journal of Iron and Steel Research International, 29(4) (2021) 1-13.
https://doi.org/10.1007/s42243-021-00648-5

[14] C.E. Aguilar-Rodriguez, J.A. Ramos-Banderas, E. Torres-Alonso, G. Solorio-Diaz, C.A. Hernández-Bocanegra, Flow characterization and inclusions removal in a slab tundish equipped with bottom argon gas feeding, Metallurgist, 61(11) (2018) 1055-1066.
https://doi.org/10.1007/s11015-018-0607-0

[15] A. Cwudziński, Numerical and physical modeling of liquid steel flow structure for one strand tundish with modern system of argon injection, Steel Research International, 88(9) (2017) 1600484.
https://doi.org/10.1002/srin.201600484

[16] A. Cwudziiiski, Mathematical simulation and water modelling of liquid steel interaction with an argon bubble curtain in a one-strand continuous casting tundish, Journal of the Southern African Institute of Mining and Metallurgy, 118(5) (2018) 544-554.
http://dx.doi.org/10.17159/2411-9717/2018/v118n5a11

[17] F. Wang, Reoxidation phenomenon and inhibition mechanism of aluminum-deoxidized steel in Tangsteel, University of Science and Technology Beijing, Beijing, 2019, p.5.

[18] R. Story Scotte, E. Goldsmith Gerry, AISTech 2006, The Association for Iron & Steel Technology, Cleveland, 2006, p. 879-889.

[19] Y.H. Sun, K.K. Cai, C.L. Zhao, Effect of transient casting operation on cleanliness of continuously cast strands, Iron Steel, 43(1) (2008) 22-25.
https://doi.org/10.13228/j.boyuan.issn0449-749x.2008.01.014

[20] Y.Q. Duan, X.H. Chen, Y.C. Wang, Causes analysis and improvements of tundish nozzle clogging for aluminized steel, Iron Steel Vanadium Titanium 36(6) (2015) 123-127. https://doi.org/10.7513/j.issn.1004-7638.2015.06.023

[21] Q.G. Liu, Y.Z. Wang, Cause analysis and improvement measures for inclusions in automobile steel DC03, China Metallurgy, 26(2) (2016) 25-30. https://doi.org/10.13228/j.boyuan.issn1006-9356.20150040

[22] L.M. Fan, Production practice of cylinder-steel 34Mn2V produced by BOF rectangular bloom CC route, Steelmaking, 26(5) (2010) 69-72.

[23] J. Gao, S.X. Yan, Z.J. Ding, Analysis on surface defects of deep-drawing piece of steel DC04-LQQ for filter and process, Special Steels, 38(4) (2017) 27-31.

[24] Y. Li, C.H. Wu, X. Xie, L. Chen, J. Chen, X.D. Yang, X.D. Ma, Numerical simulation and application of tundish cover argon blowing for a two-strand slab continuous casting machine, Metals, 12(11) (2022) 1801. https://doi.org/10.3390/met12111801

[25] L.L. Yang, Y.P. Bao, J.H. Liu, X. Dong, Y. Ren, S. Zhang, G. Xu, Investigations on metallurgical effects of tundish covering flux for continuous casting, Steelmaking, 23(2) (2007) 34-37.
https://doi.org/10.3969/j.issn.1002-1043.2007.02.010

[26] G. Miao, J.C. Wang, X.L. Liu, S.S. Sun, Development of basic covering flux for tundish, Steelmaking, 23(1) (2007) 49-52. https://doi.org/10.3969/j.issn.1002-1043.2007.01.014

[27] J. Xie, Mechanism analysis for tundish fluxes to form the solidified crusts, Journal of Materials and Metallurgy, 9(1) (2010) 15-17.
https://doi.org/10.14186/j.cnki.1671-6620.2010.01.005

[28] B. Launder, D.B. Spalding, The numerical computation of turbulent flows, Computer Methods in Applied Mechanics & Engineering, 3(2) (1974) 269-289.
https://doi.org/10.1016/B978-0-08-030937-8.50016-7

[29] X.F. Qin, C.G. Cheng, Y. Li, C.M. Zhang, J.L. Zhang, Y. Jin, A simulation study on the flow behavior of liquid steel in tundish with annular argon blowing in the upper nozzle, Metals, 9(2) (2019) 225.
https://doi.org/10.3390/met9020225

NUMERIČKA SIMULACIJA I PRIMENA UDUVAVANJA ARGONA KROZ POKLOPAC MEĐULONCA ZA KONTINUALNO LIVENJE GREDICA

C.-H. Wu [a,*], Y. Li [a], Y.-D. Liu [a], X. Xie [a], G.-R. Wu [b], M. Zhang [a]

[a] Institut za inženjerstvo i tehnologiju materijala, Istraživački institut kompanije Pangang Group, Sečuan, Kina

[b] Institut za istraživanje čelika za automobile i kućne aparate, Istraživački institut kompanije Pangang Group, Sečuan, Kina

Apstrakt

Tokom procesa kontinunualnog livenja, sadržaj preostalog kiseonika u međuloncu može se značajno smanjiti uduvavanjem argona kroz poklopac međulonca (Argon Blowing from the Tundish Cover- ABTC). Ovo može značajno poboljšati efekat zaštitnog livenja, što pomaže da se smanji reoksidacija tečnog čelika u međuloncu. U ovom radu, numerički ABTC modeli za mašine za kontinualno livenje sa šest žila su uspostavljeni i verifikovani izmerenim masenim udelom kiseonika u međuloncu tokom ABTC. Rezultati pokazuju da se najbolji uslovi za ABTC postižu postavljanjem cevi za dovod argona sa obe strane otvora na poklopcu lonca, zaptivanjem rupa za pečenje i otvorenim otvorom za čep. Brzina protoka argona treba da bude ≥120 m³/h tokom perioda praznog međulonca i ≥ 60 m³/h tokom perioda normalnog livenja. Na osnovu rezultata proračuna, izvršena su industrijska ispitivanja sa ABTC. Rezultati su pokazali da se povećani sadržaj azota u čeliku ($\Delta_{w[N]}$) smanjio za 21,5%, sa $8{,}78 \times 10^{-6}$ na $6{,}89 \times 10^{-6}$ od kraja RH do lonca, a količina inkluzija osim MnS u gredicama (veličina skeniranja: 8 mm × 8 mm) smanjena je za 21,3% sa 13,43 na 10,57, a prosečna veličina inkluzija je smanjena za 19,0%, sa 9,27 μm na 7,51 μm.

Ključne reči: Kontinualno livenje; Gredice; Međulonac; Uduvavanje argona; Čistoća; Inkluzije